

Facile Preparation of Pt^{II}-Nucleobase Monoadducts with *trans* Geometry: Structural Characterization and Kinetics for Cl⁻ Hydrolysis Reactions of *trans*-[PtCl(NH₃)₂(L-N7)]ⁿ⁺ (L = 9-Methyladenine or 9-Methylhypoxanthine)

Jorma Arpalahti,^{*,[a]} Elina Niskanen,^[b] and Reijo Sillanpää^[a]

Abstract: The employment of *trans*-[PtCl(OH)(NH₃)₂]·H₂O as the platinum source offers a convenient and efficient way to prepare 1:1 adducts with the model nucleobases 9-methyladenine (9-MeAde) and 9-methylhypoxanthine (9-MeHypH). The resulting complexes, *trans*-[PtCl(NH₃)₂(9-MeAde-N7)]ClO₄ and *trans*-[PtCl(NH₃)₂(9-MeHyp-N7)]·2H₂O, were structurally characterized by X-ray crystallography. The crystal packing of both complexes is stabilized by a hydrogen-bonding network involving primarily NH₃ ligands and perchlorate oxygens in *trans*-[PtCl(NH₃)₂-

(9-MeAde-N7)]ClO₄, and NH₃ ligands and the C(6)O group of the nucleobase in *trans*-[PtCl(NH₃)₂(9-MeHyp-N7)]·2H₂O. Three hydrogen bonds to the oxo group in the latter compound suggest that the negative charge caused by N1H deprotonation of the nucleobase is partly located on the oxygen atom; this is supported by the slightly larger downfield shift of C(6) over C(2) in the ¹³C spectrum. However, the anticipated

lengthening of the C(6)–O(6) bond upon N1H deprotonation was not verified by X-ray results. Kinetics for the Cl⁻ hydrolysis in basic aqueous solution were followed by ¹⁹⁵Pt NMR and HPLC analysis, which showed the formation of only one product in both cases with a ¹⁹⁵Pt chemical shift typical for a PtN₃O coordination sphere. The comparable kinetic data found by these two methods reveal that the water molecule acts as the nucleophile in the hydrolysis reactions and that it displaces the Cl⁻ ligand more readily in the 9-methyladenine complex.

Keywords: hydrolyses • metal ion complexes • nucleobases • platinum

Introduction

Coordination of Pt^{II} to nucleic acid constituents has been the subject of numerous studies over the past two decades.^[1] Great attention has been paid to the binding properties of Pt^{II} compounds with *cis* geometry in particular, because of the biological activity of *cis*-[PtCl₂(NH₃)₂] (cisplatin) and related compounds.^[1] By contrast, far less is known of the corresponding *trans* derivatives.^[2] However, detailed knowledge of the binding behavior of *trans*-[PtCl₂(NH₃)₂] and its structural analogues is of importance in the understanding of the factors affecting the biological activity of Pt^{II} species, together with the recent findings on the activity of various mono-^[1b, 3] and bis(platinum(II))^[4] compounds with *trans* geometry against cisplatin-resistant cell lines.

Kinetic factors in the complexation process seem to play an important role with *trans*-[PtCl₂(NH₃)₂],^[2] because of the

rather high *trans* effect of the Cl⁻ ligand.^[5] In particular, the first hydrolysis step is highly reversible,^[6] which may result in severe problems in the preparation of 1:1 adducts with nucleobases due to the insolubility of the dichloro species. Therefore, it is not surprising that only a limited number of nucleobase monoadducts with different *trans*-Pt^{II} compounds have been characterized by X-ray crystallography.^[2] In this work we report a convenient and efficient procedure for preparing 1:1 adducts with *trans*-Pt^{II}(NH₃)₂ and the model nucleobases 9-methyladenine (9-MeAde) and 9-methylhypoxanthine (9-MeHypH) by employing *trans*-[PtCl(OH)(NH₃)₂]·H₂O as the platinum source. In acidic aqueous solution this Pt^{II} species is converted to the reactive aqua species, which readily enters into complex formation.^[7] The resulting compounds, *trans*-[PtCl(NH₃)₂(9-MeAde-N7)]ClO₄ (**1**) and *trans*-[PtCl(NH₃)₂(9-MeHyp-N7)]·2H₂O (**2**), were structurally characterized by X-ray crystallography. In addition, kinetics for the Cl⁻ hydrolysis reactions of both complexes were studied in basic aqueous solution at different temperatures with ¹⁹⁵Pt NMR and HPLC analysis.

Results and Discussion

Crystal structures: The molecular structures of the cation of **1** (Figure 1) and the neutral complex of **2** (Figure 2) confirm N7

[a] Dr. J. Arpalahti, Dr. R. Sillanpää
Department of Chemistry, University of Turku
FIN-20014 Turku (Finland)
Fax: (+358)2-333-6700
E-mail: jorma.arpalahti@utu.fi

[b] E. Niskanen, MSc.
Department of Chemistry, University of Oulu
FIN-90570 Oulu (Finland)

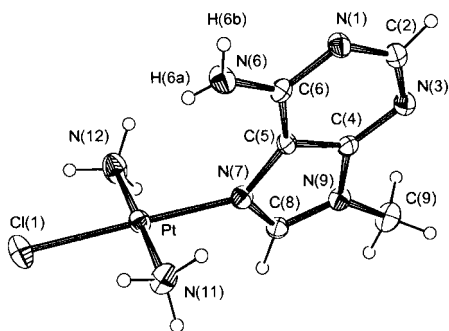


Figure 1. Molecular structure of $trans\text{-[PtCl(NH}_3)_2(9\text{-MeAde)]}^+$. Selected interatomic distances (Å) and angles ($^\circ$) with estimated deviations in parentheses: Pt–N(11) 2.054(6), Pt–N(12) 2.027(7), Pt–N(7) 2.016(5), Pt–Cl(1) 2.288(2), N(11)–Pt–N(12) 178.5(3), N(7)–Pt–N(11) 93.1(2), N(7)–Pt–N(12) 88.3(3), Cl(1)–Pt–N(7) 177.3(2), Cl(1)–Pt–N(11) 88.6(2), Cl(1)–Pt–N(12) 90.1(2).

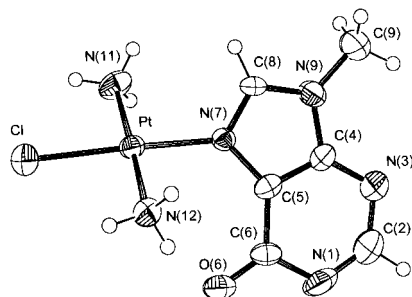


Figure 2. Molecular structure of $trans\text{-[PtCl(NH}_3)_2(9\text{-MeHyp)]}$. Selected interatomic distances (Å) and angles ($^\circ$) with estimated deviations in parentheses: Pt–N(11) 2.061(19), Pt–N(12) 2.038(19), Pt–N(7) 2.019(7), Pt–Cl 2.300(3), N(11)–Pt–N(12) 178.7(3), N(7)–Pt–N(11) 90.7(3), N(7)–Pt–N(12) 90.7(3), N(7)–Pt–Cl 176.72(18), N(11)–Pt–Cl 88.9(3), N(12)–Pt–Cl 89.8(2).

platination of both nucleobases. In both cases the Pt–N bond lengths are normal, but the angles of the platinum coordination sphere slightly deviate from the ideal square-planar geometry. Despite the charge differences on the two ligands, the bond lengths and angles of the adenine and hypoxanthine

Abstract in Finnish: *Helppo ja vaivaton tapa valmistaa tyyppiä $trans\text{-[PtCl(NH}_3)_2(L\text{-N7)]}^{n+}$ ($L = 9\text{-metyyliadeniini tai 9-metyylihypoksantiini}$) olevia komplekseja on käyttää lähtöaineenä yhdistettä $trans\text{-[PtCl(OH)(NH}_3)_2] \cdot H_2O$. Happamissa olosuhteissa HO^- ligandin protonoituessa muodostuva akvaligandi korvautuu nopeasti malliyhdisteinä käytetyillä tyyppimäksillä (nukleinihappomästen rakenneanalogeja). Valmistettujen kompleksien, $trans\text{-[PtCl(NH}_3)_2(9\text{-MeAde-N7)]-ClO}_4$ (**1**) ja $trans\text{-[PtCl(NH}_3)_2(9\text{-MeHyp-N7)]} \cdot 2H_2O$ (**2**), kiderakenne määritettiin röntgendiffraktometrisesti. Erityisen huomionarvoista on yhdisteen **2** kidehilaa stabiloiva vetysidosysteemi, jossa asemassa C(6) oleva happiatomi muodostaa kolme vetysidosta NH_3 ryhmiin. Kompleksien hydrolyysiä tutkittiin emäksisissä olosuhteissa ^{195}Pt NMR-spektroskopian ja nestekromatografian avulla. Eri menetelmillä saadut yhtäpitävät tulokset osoittavat, että nukleofiilinä toimiva vesimolekyyli korvaa Cl^- ligandin yhdisteessä **1** helpommin kuin yhdisteessä **2**.*

moieties are very similar. The packing of both complexes is stabilized predominantly by hydrogen bonding. Stacking of the nucleobases seems to be important only in **1**, where the adenine bases of the neighboring cells are weakly stacked in a head-to-tail fashion with a distance of 3.54 Å between the centers of the 5- and 6-membered rings. In **1**, both NH_3 groups form moderate or weak hydrogen bonds to the perchlorate oxygens. The two shortest nonbonded contacts are 3.022(7) Å [N(12) \cdots O(1^a)] and 3.039(8) Å [N(12) \cdots O(2^b)] [symmetry operations a) $-x+2, -y+1, -z+1$, b) $x+1, y, z$]. Furthermore, the exocyclic amino group of the adenine moiety may also participate in hydrogen bonding. One NH_2 proton [denoted as H(6B)] forms a moderate hydrogen bond to the N1 site of the neighboring cation with a distance of 3.061(8) Å [N(6) \cdots N(1^c)] (symmetry operation c) $-x+2, -y, -z+2$). In addition, the other NH_2 proton H(6A) found from the electron density maps is directed towards Pt with a distance of 2.95(8) Å (Figure 1), which may indicate weak hydrogen bonding interaction N–H \cdots Pt. In the literature, distances characteristic for this type of interaction lie within the range of 2.2–3.25 Å.^[8] For comparison, in the N7-bound adenosine complex [Pt(dien)(Ado-N7)]²⁺ the shortest possible separation for Pt^{II} and the C(6) NH_2 hydrogen was estimated as 2.83 Å.^[9]

In the crystal lattice of **2**, the neighboring nucleobase moieties are oriented in a head-to-tail fashion but the distance between the centers of the 5- and 6-membered rings is about 3.79 Å. Thus, stacking of the hypoxanthine bases does not seem to play an important role in stabilizing the crystal packing of **2**. To some extent this is unexpected since the complex is neutral, which should favor stacking. This may be attributed to deprotonation of the N1H site which leads to an increase in the electron density in the heterocyclic ring and probably causes repulsion between the base moieties. By contrast, an extensive hydrogen-bonding network stabilizes the lattice of **2** (Figure 3); the oxo group at C(6) is heavily

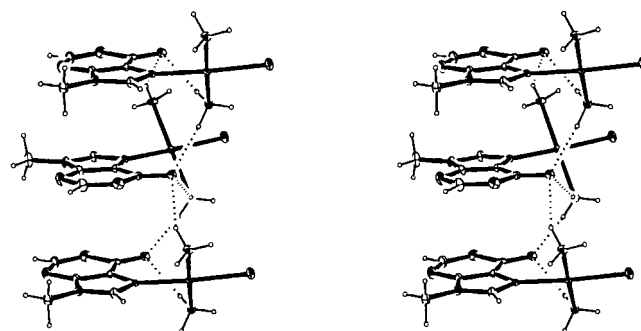


Figure 3. Stereoview showing the proposed hydrogen-bonding network in **2** (dashed lines) between the C(6)O and NH_3 groups.

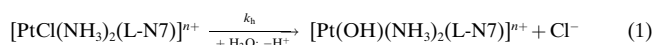
involved in hydrogen-bond formation with the ammine groups both intra- and intermolecularly [2.85(2) Å [N(12) \cdots O(6)], 2.890(13) Å [N(12) \cdots O(6^a)], 2.93(3) Å [N(11) \cdots O(6^b)]]. The water molecules are hydrogen-bonded with a distance of 2.887(13) Å [O(2) \cdots O(1)]. Other possible hydrogen bonds with water molecules are: 2.876(12) Å [O(1) \cdots N(3^a)], 3.348(11) Å [O(1) \cdots Cl^c], 3.040(12) Å

[N(12)⋯O(1^d)] [symmetry operations a) $x, -y + \frac{1}{2}, z + \frac{1}{2}$, b) $x, -y + \frac{1}{2}, z - \frac{1}{2}$, c) $x - 1, -y + \frac{1}{2}, z + \frac{1}{2}$, d) $x + 1, y, z$]. Interestingly, the existence of three rather strong hydrogen bonds to the oxo group suggests that the negative charge due to N1H deprotonation is partly located on the O(6) atom. Consequently, increasing the electron density at O(6) should reduce the double-bond character of the C(6)–O(6) bond. However, the distance of 1.252(10) Å between these atoms in **2** is within 3σ of that found in the dicationic inosine complex [Pt(dien)(Ino-N7)]²⁺, namely 1.21(2) Å.^[10] A similar situation has been reported earlier for the mixed ligand complexes of *cis*-[Pt(NH₃)₂(CG)]²⁺ and *cis*-[Pt(NH₃)₂(G–H)C]⁺ (C = 1-methylcytosine, G = 9-ethylguanine).^[11] Although Raman spectroscopy results implied a reduction in the C(6)–O(6) bond order upon G–N(1)H deprotonation, this was not definitively verified by X-ray results.^[11]

NMR studies: The ¹³C and ¹⁹⁵Pt NMR chemical shifts of **1**, **2**, and their hydrolysis products are listed in Table 1. In all cases, single ¹⁹⁵Pt resonances and sharp signals in the ¹³C spectra suggest that the dynamics of each compound in solution (i.e., rotation about the Pt–N7 bond) are fast on the NMR timescale, typical with this particular type of complex.^[12] The ¹⁹⁵Pt chemical shifts of the starting materials and reaction products are consistent with PtN₃Cl and PtN₃O coordination spheres, respectively.^[13] The assignments of the ¹³C chemical shifts given in Table 1 follow those reported for free 9-methyladenine and 9-(β-D-ribofuranosyl)hypoxanthine (inosine).^[14] In **1**, substitution of the Cl[–] ligand with an HO[–]

the hypoxanthine N1H site. In fact, a similar ¹³C chemical shift pattern has been reported in various 6-oxopurine derivatives upon N1H deprotonation.^[17] In general, a NH proton loss in N-heterocyclic compounds induces a downfield shift of the neighboring C atoms, while those more remote are only marginally shifted or display an upfield shift.^[18] In the case of 6-oxopurines, further electron removal from the 6-membered ring may be due to the electron-withdrawing effect of the oxo group, in line with the extended hydrogen-bond network involving this group as described above.

Kinetics of Cl[–] hydrolysis: In acidic aqueous solution Cl[–] hydrolysis of the compounds of the type [PtCl(NH₃)₂(L)]ⁿ⁺ (L = nucleobase) is strongly reversible; this results in a mixture of aqua and chloro species,^[6, 19] which complicates the kinetic measurements. This can be avoided by studying hydrolysis under basic conditions, since deprotonation of the aqua ligand yields a hydroxo group which, relative to the aqua ligand, can be considered inert to substitution reactions.^[7, 20, 21] Thus, the hydrolysis reactions of **1** and **2** under basic conditions may be described by Equation (1). Note that at pH 10–12, the former exists as a monocation while the latter is a neutral species.



In both cases, the ¹⁹⁵Pt NMR spectra and HPLC traces of the reaction mixtures revealed the formation of only a single Pt-nucleobase adduct during hydrolysis (Figures 4 and 5). Observed rate constants obtained by Equation (2) from the disappearance of the starting material and from the formation of the product were compatible in all cases (Table 2). The similarity of the values found for k_h by ¹⁹⁵Pt NMR and by

Table 1. ¹³C and ¹⁹⁵Pt NMR chemical shifts of **1**, **2**, and their hydrolysis products.^[a]

Compound	$\delta_{\text{Pt}}^{[b]}$	$\delta_{\text{C}}^{[c]}$					
		C(2)	C(4)	C(5)	C(6)	C(8)	C(9)
1 ^[d]	–2330	153.5	148.5	115.7	154.0	144.7	30.8
1 ^[e]	–2040	153.3	148.5	116.1	154.1	145.2	30.7
2 ^[d]	–2280	147.3	148.3	121.1	156.3	144.5	31.1
2 ^[e]	–1990	154.2	148.9	120.6	165.2	142.7	30.3

[a] Spectra recorded in water. [b] Chemical shift from external Na₂[PtCl₆]. [c] Chemical shift from TMS. [d] At pH 5. [e] After complete hydrolysis at pH > 10.

group in the Pt coordination sphere at pH 11 causes no significant changes in the ¹³C chemical shifts of the nucleobase. The largest effect is seen at C(5) and C(8) with a downfield shift of 0.4 and 0.5 ppm, respectively. The situation is markedly different for compound **2**. The C(2) and C(6) signals show large downfield shifts of 6.9 and 8.9 ppm, respectively, while C(4) is shifted downfield only slightly by 0.6 ppm. By contrast, the C(5), C(8) and C(9) signals display upfield shifts of 0.5, 1.8, and 0.8 ppm, respectively. In the pH range 5–11, **1** has no dissociable proton (a $\text{p}K_a > 13$ has been reported^[15] for the exocyclic amino group in N7-platinated 9-MeAde). By contrast in **2**, Pt^{II} binding to the N7 site of 9-MeHyp lowers the $\text{p}K_a$ of N1H (ca. 9.5) by approximately 1.5 log units.^[16] Thus, the changes in ¹³C chemical shifts following the hydrolysis reaction of **2** [PtN₃Cl (pH 5) → PtN₃O (pH 11)] must be attributed to the deprotonation of

Table 2. Observed rate constants for the hydrolysis of **1** and **2** in basic aqueous solution (pH ~ 10).^[a]

Compound	T [K]	k_h [10 ^{–5} s ^{–1}]	
		[b]	[c]
1	303.2	6.50 ± 0.05	6.54 ± 0.04
		8.2 ± 0.4 ^[d]	8.7 ± 0.2 ^[d]
	313.2	18.2 ± 0.02	17.9 ± 0.02
2	323.2	52.1 ± 0.4	53 ± 1
	303.2	1.80 ± 0.03	1.83 ± 0.06
		1.91 ± 0.04 ^[d]	1.80 ± 0.06 ^[d]
	313.2	6.03 ± 0.09	5.76 ± 0.09
	323.2	17.7 ± 0.1	18.4 ± 0.1
	17.8 ± 0.2 ^[e]	18.4 ± 0.4 ^[e]	
		16 ± 1 ^[f]	

[a] $I = 0.1\text{M}$ (NaClO₄); data obtained by HPLC unless otherwise indicated. [b] From the disappearance of the starting material. [c] From the formation of the product. [d] Data obtained by ¹⁹⁵Pt NMR, $T = 303 \pm 1\text{K}$, at ambient ionic strength. [e] At pH 12.1. [f] Initial rate constant at pH 3.06, the concentration of **2** was $1.0 \times 10^{-5}\text{M}$.

HPLC analysis supports the validity of the data and exemplifies the usefulness of ¹⁹⁵Pt NMR for kinetic studies. In this particular case, the ¹⁹⁵Pt NMR method offered a more pronounced way to follow the substitution reaction because of the rather poor resolution between the starting material and the reaction product in the HPLC analysis (cf. Figures 4 and 5).

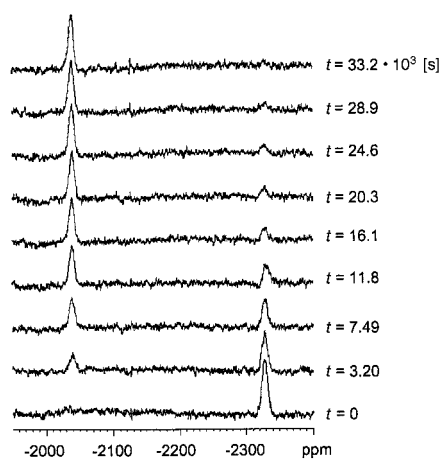


Figure 4. Time-dependent ^{195}Pt NMR spectra of the hydrolysis of $\text{trans-}[\text{PtCl}(\text{NH}_3)_2(9\text{-MeAde})]^+$ in basic aqueous solution ($\text{pH} > 10$). The times denoted indicate the midpoints of acquisitions (in 10^3 s).

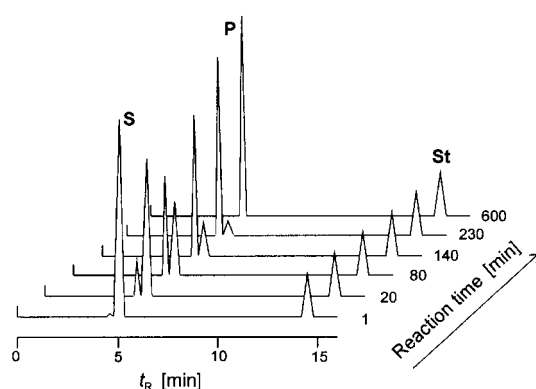


Figure 5. HPLC traces of the hydrolysis of $\mathbf{2}$ (5×10^{-5} M) in basic aqueous solution ($\text{pH} 10$, $T = 323.2$ K) with aqueous NaClO_4 (0.05 M, $\text{pH} 3$) as an eluent with a flow rate of 0.7 mL min^{-1} . Notation: **S**, starting material; **P**, product; **St**, internal standard (1 -methyluracil, 2×10^{-5} M).

Mechanistically, both Cl^- hydrolysis reactions seem to obey an associative mechanism, as indicated by the activation parameters $\Delta H^\ddagger = 83 \pm 2$ kJ mol^{-1} and $\Delta S^\ddagger = -52 \pm 5$ $\text{J K}^{-1} \text{mol}^{-1}$ for $\mathbf{1}$, and $\Delta H^\ddagger = 91 \pm 1$ kJ mol^{-1} and $\Delta S^\ddagger = -37 \pm 4$ $\text{J K}^{-1} \text{mol}^{-1}$ for $\mathbf{2}$. Almost identical values found for the hydrolysis reactions of $\mathbf{2}$ at $\text{pH} 10$ and 12 (Table 2) imply that it is the water molecule rather than the HO^- ion which is the nucleophile in these reactions. Quite interestingly, the Cl^- hydrolysis rate for $\mathbf{1}$ is about three times faster than for $\mathbf{2}$, in spite of the more basic nature of the hypoxanthine N7 site.^[22] It is worth noting that the initial rate constant for the hydrolysis of $\mathbf{2}$ at $\text{pH} 3.0$ is comparable to the hydrolysis rate constant at higher pH (Table 2). In addition, the value of $(1.04 \pm 0.03) \times 10^{-4} \text{ s}^{-1}$ calculated for the hydrolysis rate constant of $\mathbf{2}$ at 318.2 K with the Arrhenius equation^[23] is close to that reported earlier for the corresponding monocationic inosine complex $\text{trans-}[\text{PtCl}(\text{NH}_3)_2(\text{InoH-N7})]^+$, namely $(9.4 \pm 0.7) \times 10^{-5} \text{ s}^{-1}$ at 318.2 K.^[6] Thus, deprotonation of the N1H in the 6-oxopurine moiety does not significantly affect the Cl^- hydrolysis rate in $\text{trans-Pt}^{\text{II}}$ complexes, although increased electron density of the heteroaromatic ring due to the proton loss [cf. the upfield shift of C(8)] might have been anticipated to strengthen the *trans* effect of the N7 site and

result in faster Cl^- hydrolysis. This suggests that the ability of the nucleophile (i.e., the water molecule) to attack Pt^{II} plays an important role. Thus, the retarded rate for the Cl^- hydrolysis of $\mathbf{2}$ may be a result of the charge differences of the complexes and/or the accumulation of negative charge on the oxygen atom at C(6) close to Pt^{II} (vide supra) making $\mathbf{2}$ a less attractive target for the incoming water molecule.

Conclusion

The employment of $\text{trans-}[\text{PtCl}(\text{OH})(\text{NH}_3)_2] \cdot \text{H}_2\text{O}$ as the platinum source offers a convenient and efficient way to prepare N7 bound 1:1 complexes with the model nucleobases 9-methyladenine and 9-methylhypoxanthine. The X-ray crystal structures of the resulting complexes confirm N7 platination in both cases. The crystal packing of both complexes is stabilized by a hydrogen-bonding network involving primarily NH_3 ligands and perchlorate oxygens in $\text{trans-}[\text{PtCl}(\text{NH}_3)_2(9\text{-MeAde-N7})]\text{ClO}_4$, and NH_3 ligands and the C(6)O group of the nucleobase in $\text{trans-}[\text{PtCl}(\text{NH}_3)_2(9\text{-MeHyp-N7})] \cdot 2\text{H}_2\text{O}$. Three hydrogen bonds to the oxo group in the latter compound suggest that the negative charge as a result of N1H deprotonation of the nucleobase is partly located on the oxygen atom, which is supported by the larger downfield shift of C(6) over C(2) in the ^{13}C spectrum of this species. Unfortunately, lengthening of the C(6)–O(6) bond upon N1H deprotonation was not verified by X-ray results. Kinetics for the Cl^- hydrolysis in basic aqueous solution were followed by ^{195}Pt NMR and HPLC analysis, which showed the formation of only one product in both cases with a ^{195}Pt chemical shift typical for a PtN_3O coordination sphere. The comparable kinetic data found by these two methods reveal that the water molecule acts as the nucleophile in the hydrolysis reactions and that it displaces the Cl^- ligand more readily in the 9-methyladenine complex.

Experimental Section

Materials: 9-Methylhypoxanthine (9-MeHypH) from Chemogen was used as received. The compounds 9-methyladenine^[24] (9-MeAde) and $\text{trans-}[\text{PtCl}(\text{OH})(\text{NH}_3)_2] \cdot \text{H}_2\text{O}$ ^[25] were prepared by literature methods. For the preparation of $\text{trans-}[\text{PtCl}(\text{NH}_3)_2(9\text{-MeAde-N7})]\text{ClO}_4$ ($\mathbf{1}$), $\text{trans-}[\text{PtCl}(\text{OH})(\text{NH}_3)_2] \cdot \text{H}_2\text{O}$ (72.5 mg, 0.24 mmol) was dissolved in water (1.0 mL) and added to a solution of 9-methyladenine (38 mg, 0.26 mmol) in HClO_4 (1 mL, 1 M) (Pt^{II} coordination to the N1 site of 9-MeAde is prevented in strongly acidic solution^[9]). After stirring for 5 min at ambient temperature and for 1 min at 60°C the mixture was cooled on ice to yield a white precipitate. Presumably $\mathbf{1}$ precipitates under these conditions as a hydroperchlorate, but it may also contain water of crystallization. The precipitate was filtered, washed first with ice-cold water (2 mL) and then with acetone, and finally air-dried. Yield: 110 mg ($\sim 75\%$, as hydroperchlorate). The dried precipitate (approx. 20 mg) was dissolved in NaOH (2 mL, 0.0125 M) by gentle warming to give a clear solution ($\text{pH} \sim 4$). Compound $\mathbf{1}$ crystallized from the solution as thin colorless plates after storage in a refrigerator. The remainder of the solid substance was dissolved in sufficient amount of NaOH (1 M) solution to give a neutral solution. After precipitation on ice, $\mathbf{1}$ was filtered, washed with cold water, and acetone, and finally air-dried.

$\text{trans-}[\text{PtCl}(\text{NH}_3)_2(9\text{-MeHypH-N7})]\text{ClO}_4$ ($\mathbf{2a}$) was obtained in a similar manner by a 1:1 reaction between $\text{trans-}[\text{PtCl}(\text{OH})(\text{NH}_3)_2] \cdot \text{H}_2\text{O}$ (0.32 mmol) and 9-methylhypoxanthine (48 mg, 0.32 mmol) with 1.5 equiv-

alent of HClO₄ (0.5 M), which gave 117 mg (72%) of **2a** as very thin, colorless needles. The crude product (approx. 20 mg) dissolved in water (1 mL) followed by the addition of 1.5 equivalent NaOH (1 M) afforded colorless plates of *trans*-[PtCl(NH₃)₂(9-MeHyp-N7)]·2H₂O (**2**) after storage in a refrigerator and which easily lost water of crystallization. A selected piece of crystal was sealed in a capillary to avoid decomposition of **2** during X-ray measurement.

Kinetic measurements by HPLC: The hydrolysis of **1** and **2** in basic aqueous solution (pH 9.5–12) at different temperatures was studied with HPLC as an analytical tool. Kinetic runs were started by adding the desired amount of the complex to a prethermostatted reaction mixture, the ionic strength of which was adjusted to 0.1 M with NaClO₄. Samples withdrawn from the reaction mixture at suitable time intervals were diluted with ice-cold HClO₄ (0.01 M, 1:1), and immediately analyzed by HPLC with an RP-18 column (Merck LiChrospher 100 endcapped, 5 μm) and aqueous NaClO₄ (0.05 M, pH 3) as an eluent. Peak areas at 260 nm were used as the measure of the concentration by employing 1-methyluracil as an internal standard.

First-order rate constants k_t for the disappearance of the starting material were obtained with Equation (2), where $[MCl]_0$ denotes the initial concentration of the chlorocomplex and $[MCl]_t$ is the concentration at time t .

$$\ln[MCl]_t = -k_t t + [MCl]_0 \quad (2)$$

Substitution of the terms $[MCl]_t$ and $[MCl]_0$ in Equation (2) with $([MOH]_{\infty} - [MOH]_t)$ and $[MOH]_{\infty}$, respectively, enabled calculation of the rate constants from the formation of the aqua species (the term $[MOH]_{\infty}$ denotes the final concentration of the aqua species). All reactions were followed for at least two half-lives; this provided strictly linear plots of $\ln[L]_t$ [or $\ln([MOH]_{\infty} - [MOH]_t)$] vs. t in each case.

NMR studies: The ¹⁹⁵Pt NMR spectra were recorded on a Bruker DPX 400 instrument equipped with a variable temperature unit at 85.6 MHz ($T = 303$ K), with external Na₂[PtCl₆] as the chemical shift reference ($\delta = 0$). The samples were prepared by dissolving 20 mg of **1** or **2a** in distilled water (2.5 mL) to obtain the reference spectrum and by adding 1.2 or 3.0 equiv of NaOH, respectively, for hydrolysis. For each spectrum of **1** and **2**, 4000 and 8000 scans, respectively, were collected giving accumulation times of 36 min and 72 min. Exponential line broadening (50 Hz) was applied prior to FT followed by automatic baseline correction which was applied prior to manual integration. In ¹⁹⁵Pt NMR kinetic studies integrated peak areas were used to measure the concentration, and the midpoints of the measuring time interval for each spectrum were taken as the measurement time.^[26] The rate constants were obtained using Equation (2). The ¹³C{¹H} spectra of both complexes were recorded before and after hydrolysis at 100.6 MHz ($T = 303$ K) with external acetone as the chemical shift reference ($\delta(^{13}\text{C}) = 30.7$ from TMS at $\delta = 0$).

X-ray diffraction studies: All X-ray data were collected on a Rigaku AFCSS diffractometer at ambient temperature with MoK_α radiation ($\lambda = 0.71069$ Å). Unit cell parameters were obtained from a least-squares fit of 25 reflections ($25.78 < 2\theta < 29.58^\circ$ (**1**) and $37.95 < 2\theta < 45.35^\circ$ (**2**)). Intensity data were collected by the $\omega/2\theta$ scan technique to a maximum 2θ value of 50° . The intensities of three standard reflections were measured every 150 data points, and a linear correlation was applied to account for the intensity decay (**2**). The intensities of the reflections were corrected for Lorenz, polarization and absorption (empirical) effects.^[27] The structures were solved by standard Patterson and difference Fourier methods and refined by full-matrix least-squares calculations employing SHELXL-97.^[28] In both **1** and **2**, all atoms except hydrogen were refined with anisotropic temperature factors. In **1**, the NH₃ and CH₃ hydrogens are at the calculated positions, while the NH₂ and the ring hydrogens were found from the electron-density maps and were refined with fixed displacement factors. In **2**, only the water hydrogens were found from the electron-density maps and were refined; others are at the calculated positions. The final cycle of refinement for the structure **1** gave $R1 = 0.0265$ and $wR2 = 0.0545$ for the observed data [$I > 2\sigma(I)$] and 194 parameters and $R1 = 0.0369$ and $wR2 = 0.0570$ for all data. For **2** refinement converged at $R1 = 0.0298$ and $wR2 = 0.0544$ for the observed data and 166 parameters and $R1 = 0.0694$ and $wR2 = 0.0619$ for all data. Crystallographic data and experimental details are given in Table 3; selected bond lengths and angles are given in Figures 1

Table 3. Crystal data and data collection parameters for the structures of *trans*-[PtCl(NH₃)₂(9-MeAde-N7)]ClO₄ (**1**) and *trans*-[PtCl(NH₃)₂(9-MeHyp-N7)]·2H₂O (**2**).

	1	2
formula	C ₆ H ₁₃ N ₇ O ₄ Cl ₂ Pt	C ₆ H ₁₅ N ₆ O ₃ ClPt
M_r	513.21	449.78
system	triclinic	monoclinic
space group	$P\bar{1}$ (no. 2)	$P2(1)/c$ (no. 14)
a [Å]	8.491(2)	11.101(2)
b [Å]	12.158(2)	15.690(2)
c [Å]	7.450(2)	7.496(3)
α [°]	98.68(2)	90
β [°]	113.70(2)	104.58(2)
γ [°]	84.49(2)	90
V [Å ³]	695.6(3)	1263.6(5)
Z	2	4
ρ_{calcd} [Mg m ⁻³]	2.450	2.364
absorb. coeff. [mm ⁻¹]	10.495	11.324
crystal size [mm]	0.10 × 0.08 × 0.06	0.20 × 0.18 × 0.14
measured reflns	2626	2500
unique reflns	2445	2218
observed reflns	2445	2218
$T_{\text{min}}, T_{\text{max}}$	0.442, 1.000	0.362, 1.000
variation obs. stand.		−3.6%
decay correction		linear
refinement type	on F^2	on F^2
$R1$ [$I > 2\sigma(I)$] ^[a]	0.0265	0.0298
$wR2$ [$I > 2\sigma(I)$] ^[b]	0.0545	0.0544
GoF (= S) ^[c]	1.028	1.008
parameters refined	194	166
$(\Delta\rho)_{\text{min}}$ [e Å ⁻³]	−0.660	−0.614
$(\Delta\rho)_{\text{max}}$ [e Å ⁻³]	0.943	0.835

[a] $R1 = \sum ||F_o| - F_c| / \sum |F_o|$. [b] $wR2 = \{\sum [w(F_o^2 - F_c^2)^2] / \sum [w(F_o^2)^2]\}^{1/2}$ and $w = 1 / [\sigma^2(F_o^2) + (aP)^2 + (bP)]$, where $P = (2F_o^2 + F_c^2) / 3$. [c] $\{\sum [w(F_o^2 - F_c^2)^2] / (n - p)\}^{1/2}$, where $n = \text{no. of reflns}$ and $p = \text{no. of refined parameters}$.

and **2**. Data reduction and subsequent calculations were performed with teXsan for Windows.^[29] Figures were drawn with ORTEP-3 for Windows.^[30] Crystallographic data (excluding structure factors) for the structures reported in this paper have been deposited with the Cambridge Crystallographic Data Centre as supplementary publication no. CCDC-111918, CCDC-111919. Copies of the data can be obtained free of charge on application to CCDC, 12 Union Road Cambridge, CB2 1EZ, UK (Fax: (+44) 1223-336-033; e-mail: deposit@ccdc.cam.ac.uk).

Acknowledgment

Financial support from the Tauno Tönning Foundation (E.N.) is gratefully acknowledged. This work is a part of the COST Action D8/004/97 (Chemistry of Metals in Medicine).

- [1] For recent reviews, see e. g.: a) J. Arpalahti, *Met. Ions Biol. Syst.* **1996**, 32, 379–395; b) N. Farrell, *Met. Ions Biol. Syst.* **1996**, 32, 603–639; c) M. J. Bloemink, J. Reedijk, *Met. Ions Biol. Syst.* **1996**, 32, 641–685; d) J. Reedijk, *Chem. Commun.* **1996**, 801–806.
- [2] B. Lippert, *Met. Ions Biol. Syst.* **1996**, 33, 105–141.
- [3] a) M. Coluccia, A. Nassi, F. Loseto, A. Boccarelli, M. A. Mariggio, D. Giordano, F. P. Intini, P. Caputo, G. Natile, *J. Med. Chem.* **1993**, 36, 510–512; b) M. Coluccia, A. Boccarelli, M. A. Mariggio, N. Cardellicchio, P. Caputo, F. P. Intini, G. Natile, *Chem. Biol. Interact.* **1995**, 98, 251–266.
- [4] N. Farrell, Y. Qu, M. P. Hacker, *J. Med. Chem.* **1990**, 33, 2179–2184.
- [5] R. G. Wilkins, *Kinetics and Mechanism of Reactions of Transition Metal Complexes*, 2nd ed., VCH, Weinheim, **1991**, p. 237.
- [6] M. Mikola, J. Arpalahti, *Inorg. Chem.* **1994**, 33, 4439–4445.

- [7] M. Mikola, P. Oksman, J. Arpalahti, *J. Chem. Soc. Dalton Trans.* **1996**, 3101–3104.
- [8] a) W. Yao, O. Eisenstein, R. H. Crabtree, *Inorg. Chim. Acta* **1997**, 254, 105–111; b) D. Braga, F. Grepioni, E. Tedesco, K. Biradha, G. R. Desiraju, *Organometallics* **1997**, 16, 1846–1856.
- [9] J. Arpalahti, K. D. Klika, R. Sillanpää, R. Kivekäs, *J. Chem. Soc. Dalton Trans.* **1998**, 1397–1402.
- [10] R. Melanson, F. D. Rochon, *Acta Crystallogr. Sect. B: Struct. Sci.* **1978**, 34, 3594–3598.
- [11] R. Faggiani, B. Lippert, C. J. L. Lock, R. A. Speranzini, *Inorg. Chem.* **1982**, 21, 3216–3225.
- [12] M. D. Reily, L. G. Marzilli, *J. Am. Chem. Soc.* **1986**, 108, 6785–6793.
- [13] T. G. Appleton, J. R. Hall, S. F. Ralph, *Inorg. Chem.* **1985**, 24, 4685–4693.
- [14] M.-T. Chenon, R. J. Pugmire, D. M. Grant, R. P. Panzica, L. B. Townsend, *J. Am. Chem. Soc.* **1975**, 97, 4627–4636.
- [15] B. Lippert, *Progr. Inorg. Chem.* **1989**, 37, 1–97.
- [16] J. H. J. den Hartog, M. L. Salm, J. Reedijk, *Inorg. Chem.* **1984**, 23, 2001–2005.
- [17] L. G. Marzilli, B. de Castro, C. Solorzano, *J. Am. Chem. Soc.* **1982**, 104, 461–466.
- [18] a) R. J. Pugmire, D. M. Grant, *J. Am. Chem. Soc.* **1971**, 93, 1880–1887; b) E. Breitmaier, K.-H. Spohn, *Tetrahedron* **1973**, 29, 1145–1152.
- [19] J. Arpalahti, M. Mikola, S. Mauristo, *Inorg. Chem.* **1993**, 32, 3327–3332.
- [20] J. Arpalahti, *Inorg. Chem.* **1990**, 29, 4598–4602.
- [21] M. Mikola, J. Arpalahti, *Inorg. Chem.* **1996**, 35, 7556–7562.
- [22] R. B. Martin, *Met. Ions Biol. Syst.* **1996**, 32, 61–89.
- [23] $\ln k_h = 26.03 - 93.11/RT$
- [24] H. Lönnberg, J. Ylikoski, J. Arpalahti, E. Ottoila, A. Vesala, *Acta Chem. Scand.* **1985**, A39, 171–180.
- [25] J. Arpalahti, R. Sillanpää, M. Mikola, *J. Chem. Soc. Dalton Trans.* **1994**, 1499–1500.
- [26] M. Becker, R. E. Port, H.-J. Zabel, W. J. Zeller, P. Bachert, *J. Magn. Res.* **1998**, 113, 115–122.
- [27] A. C. T. North, D. C. Phillips, F. S. Mathews, *Acta Crystallogr. Sect. A: Found. Crystallogr.* **1968**, 24, 351–359.
- [28] G. M. Sheldrick, *SHELXL 97, Program for the Refinement of Crystal Structures*, University of Göttingen, **1997**.
- [29] *teXsan for Windows. Structure Analysis Software*. Molecular Structure Corporation, TX 77381, USA, **1997**.
- [30] L. J. Farrugia, *J. Appl. Crystallogr.* **1997**, 30, 565.

Received: December 3, 1998 [F 1475]